Bone Morphogenetic Protein-2 Rapidly Heals Two Distinct Critical Sized Segmental Diaphyseal Bone Defects in a Porcine Model

Todd O. McKinley, MD; Paul Childress, PhD†; Emily Jewell, MD‡; Kaitlyn S. Griffin, MD§; Austin E. Wininger, MD‖; Aamir Tucker, BS¶; Adam Gremah, BS¶; Michael K. Savaglio, BS¶; Stuart J. Warden, PhD**; Robyn K. Fuchs, PhD**; Roman M. Natoli, MD, PhD*; Karl D. Shively, MD*; Jeffrey O. Anglen, MD††; Tien-Min Gabriel Chu, DDS‡‡; Melissa A. Kacena, PhD**

ABSTRACT

Introduction:

Segmental bone defects (SBDs) are devastating injuries sustained by warfighters and are difficult to heal. Preclinical models that accurately simulate human conditions are necessary to investigate therapies to treat SBDs. We have developed two novel porcine SBD models that take advantage of similarities in bone healing and immunologic response to injury between pigs and humans. The purpose of this study was to investigate the efficacy of Bone Morphogenetic Protein-2 (BMP-2) to heal a critical sized defect (CSD) in two novel porcine SBD models.

Materials and Methods:

Two CSDs were performed in Yucatan Minipigs including a 25.0-mm SBD treated with intramedullary nailing (IMN) and a 40.0-mm SBD treated with dual plating (ORIF). In control animals, the defect was filled with a custom spacer and a bovine collagen sponge impregnated with saline (IMN25 Cont, $n = 8$; ORIF40 Cont, $n = 4$). In experimental animals, the SBD was filled with a custom spacer and a bovine collage sponge impregnated with human recombinant BMP-2 (IMN25 BMP, $n = 8$; ORIF40 BMP, $n = 4$). Healing was quantified using monthly modified Radiographic Union Score for Tibia Fractures (mRUST) scores, postmortem CT scanning, and torsion testing.

Results:

BMP-2 restored bone healing in all eight IMN25 BMP specimens and three of four ORIF40 BMP specimens. None of the IMN25 Cont or ORIF40 Cont specimens healed. mRUST scores at the time of sacrifice increased from 9.2 ($\pm$2.4) in IMN25 Cont to 15.1 ($\pm$1.0) in IMN25 BMP specimens ($P < .0001$). mRUST scores increased from 8.2 ($\pm$1.1) in ORIF40 Cont to 14.3 ($\pm$1.0) in ORIF40 BMP specimens ($P < .01$). CT scans confirmed all BMP-2 specimens had healed and none of the control specimens had healed in both IMN and ORIF groups. BMP-2 restored 114% and 93% of intact torsional stiffness in IMN25 BMP and ORIF40 BMP specimens.

Conclusions:

We have developed two porcine CSD models, including fixation with IMN and with dual-plate fixation. Porcine models are particularly relevant for SBD research as the porcine immunologic response to injury closely mimics the human response. BMP-2 restored healing in both CSD models, and the effects were evident within the first month after injury. These findings support the use of both porcine CSD models to investigate new therapies to heal SBDs.

INTRODUCTION

Segmental bone defects (SBDs) are most often the result of high-energy extremity trauma.[1,2] SBDs are at high risk to develop nonunion reflected by ongoing intensive research to develop methods to treat SBDs.[3,4] Warfighters are at risk of sustaining severe composite extremity injuries that typically include SBDs.[5] Critical to investigating treatments is access to relevant translational models that accurately simulate anatomic and physiologic human conditions resulting from SBDs. Relevant large animal models optimally simulate human bone biology and immunologic response to injury and reproduce forces encountered in humans during fracture healing.[6] To date, the most commonly used large animal models for SBD research are sheep, goats, and dogs.[7–13] Interestingly, bone composition and bone remodeling in pigs more closely resembles humans compared to dogs and sheep.[14] In addition, the porcine immunologic response to injury and hemorrhage closely mimics humans,[15–17] which is relevant

*Department of Orthopaedic Surgery, Indiana University School of Medicine, Indianapolis, IN 46202, USA

†Anagin Inc, Indianapolis, IN 46202, USA

‡Hand Surgery Associates of Indiana, Indianapolis, IN 46260, USA

§Department of Obstetrics and Gynecology, University of Cincinnati School of Medicine, Cincinnati, OH 45267, USA

‖Department of Orthopaedic Surgery, Methodist Hospital, Houston, TX 77030, USA

¶Marian University College of Osteopathic Medicine, Indianapolis, IN 46222, USA

**Department of Physical Therapy, Indiana University School of Health and Human Sciences, Indianapolis, IN 46202, USA

††Sadhana Boneworks, Indianapolis, IN 46220, USA

‡‡Indiana University School of Dentistry, Indianapolis, IN 46202, USA

doi:https://doi.org/10.1093/milmed/usab360

because many SBDs occur in polytraumatized patients.[18] However, porcine SBD models are pragmatically scarce primarily due to excessive body weight in pigs. Taken together, there is a paucity of research using porcine models that have the potential to better simulate human bone healing compared to traditional large animal models.

We have developed a porcine SBD model using Yucatan minipigs (YMPs).[19] Yucatan minipigs offer distinct advantages as a preclinical SBD model, including similar bone physiology, bone healing, and remarkably similar immunologic response to injury compared to humans.[15–17,20,21] In addition, full-grown YMPs range from 60 to 100 kg. In model development, we demonstrated that a 25.0-mm SBD in the mid-tibial diaphysis healed when stabilized with dual orthogonal plating (ORIF) but did not heal when stabilized with an intramedullary nail (IMN).[19] We also demonstrated that a 40.0-mm SBD stabilized with dual orthogonal plating also failed to heal. Taken together, we identified two critical sized defects (CSDs) in a load-bearing porcine diaphyseal model, which afford opportunities to investigate interventions.

Multiple strategies have been used to heal SBDs that include autografts, allografts, cell-based augmentation, and augmentation with osteoinductive molecules.[22,23] Recombinant human Bone Morphogenetic Protein-2 (BMP-2; INFUSE, Medtronic Inc, Minneapolis, MN) has been the most extensively studied augmentation strategy, and it has demonstrated success in small[24–26] and large[8,13] animal models. The purpose of this study was to test the efficacy of BMP-2 in our two established porcine CSD models to further validate the relevance of our porcine diaphyseal CSD model. We hypothesized that BMP-2 would restore bone healing in both models. Experimental groups of pigs subjected to a 25.0-mm SBD treated with IMN and subjected to a 40.0-mm defect treated with ORIF were treated with BMP. These results were compared to our original corresponding models that were untreated and developed nonunions.

METHODS

Experimental Protocol

Our protocol and methods were approved by the U.S. Army Medical Research and Development Command Animal Care and Use Review Office and subsequently by our Institutional Animal Care and Use Committee. Two experimental groups were investigated and compared to our CSD YMPs that had been originally investigated in model development.[19] One set of YMPs were subjected to a 25.0-mm mid-diaphyseal tibial SBD and stabilized with a custom-designed intramedullary nail (IMN25; Fig. 1). The SBD was filled with a custom-fabricated polypropylene fumarate/tricalcium phosphate (PPF/TCP) scaffold spacer[24] circumfrentially wrapped a type I bovine collagen sponge. In the original control animals[19] (IMN25 Cont; $n = 8$), the sponge was impregnated with 1.5 mL of saline. In experimental animals, the sponge was impregnated with 1.5 mg of BMP-2 in 1.5 mL of saline (IMN25 BMP; $n = 8$). The other set of YMPs was subjected to a 40.0-mm tibial diaphyseal SBD and stabilized with dual plating (ORIF40; Fig. 1). The defect was filled with a custom PPF/TCP scaffold spacer and a collagen sponge. In original control animals,[19] the sponge was impregnated with 1.5 mL of saline (ORIF40 Cont; $n = 4$), and in experimental animals, the sponge was impregnated with 1.5 mg of BMP-2 in 1.5 mL of saline (ORIF40 BMP; $n = 4$). Pigs were returned to routine cage activity. Intramedullary nail pigs were followed for 6 months. ORIF pigs were followed for 3 months.

SURGERY

Pigs were induced with intravenous telazole, ketamine, and xylazine and maintained under anesthesia with isoflurane

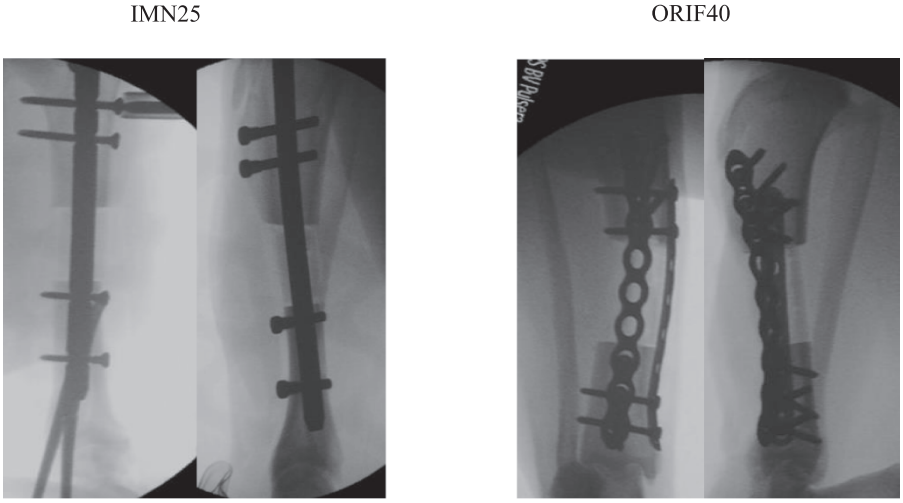

FIGURE 1. Two segmental bone defect models with critical sized defects were studied. Postoperative intramedullary nail (IMN25) X-rays are shown on the left, and dual-plating (ORIF40) X-rays are shown on the right.

during surgery. Ceftiofur, 5 mg/kg, was administered before incision for antimicrobial prophylaxis. The right hind limb was shaved and scrubbed with tricolsan followed by 70% ethanol. The surgical site was then prepared with betadine and draped in a sterile fashion.

Intramedullary Nailing[19]

A 4.0-cm skin incision medial to the patella and a medial parapatellar arthrotomy afforded access to the top of the tibial plateau. A 4.0-mm Steinmann pin was inserted into the medullary canal, and its position was confirmed with fluoroscopy. Subsequently, hand reamers were sequentially inserted through the opening pin tract and through the entire length of the tibia to a diameter of 9 mm. A custom-designed 120-mm-long, 8-mm diameter stainless steel IMN (Medical Innovations International Inc., Rochester, MN) was inserted into the canal, and the position was verified with fluoroscopy. Once proper fit and position were confirmed, the IMN was removed.[19]

A 6.0-cm skin incision, starting 2 cm proximal to the distal end of the palpable tibial tubercle, was carried sharply down onto the anterior tibia. Sharp dissection was carried deep between the bone and adjacent muscle, and the tibia was circumferentially exposed. Two parallel transverse osteotomies were made 25.0 mm apart. The proximal end of the osteotomy was made 3 mm below the inferior most aspect of the tibial tubercle. The SBD was created, and the intercalated spacer was inserted into the defect. The scaffold was a PPF/TCP scaffold with a 20-mm outer diameter, 12-mm inner diameter, and 25-mm height fabricated using casting methods described previously.[24] The IMN was then re-inserted through the central canal of the scaffold and into its final position in the tibia. The IMN was statically locked with two 3.5-mm crosslock screws in the proximal tibia and two 3.5-mm crosslock screws in the distal tibia.[19]

An FDA-approved type I bovine collagen sponge (Helistat, 7.5 cm × 5.0 cm × 5.0 mm), which was treated with either 1.5 mg human recombinant BMP-2 (IMN25 BMP; $n = 8$) solubilized in 1.5 mL sterile saline or 1.5 mL of saline alone (IMN25 Cont; $n = 8$) was placed circumferentially around the scaffold and secured with 3.0 Vicryl suture to local tissue. Care was taken to ascertain that the sponge contacted both the proximal and distal bone in the defect. The fascia and subcuticular layer were closed with 3.0 Vicryl suture. The skin was closed with 2-0 Vicryl suture. Pigs were returned to routine cage activity.

Open Reduction with Internal Fixation[19]

In the ORIF40 YMPs, a 14.0-cm incision was made beginning from the proximal lateral leg lateral to the palpable border of the tibia and then curving medial to parallel the palpable anterior border of the tibia. Sharp dissection came directly down over the bone. A nine-hole 3.5-mm dynamic compression plate was contoured to rest on the lateral surface of the tibia and was secured to the intact bone with a single 3.5-mm screw above and below the SBD resection site. A second eight-hole one-third tubular plate was laid against the medial tibial surface and secured with a single 3.5-mm screw above and below the SBD resection site. The one-third tubular plate was then removed to allow access to the lateral surface of the bone for resection. The 40.0-mm resection was measured and marked, and then cuts were made with an oscillating saw. Immediately after resecting the bone, the defect was stabilized by securing both plates. We used six 3.5-mm screws (three above and three below the SBD) in the dynamic compression plate and four screws (two above and two below the SBD) in the one-third tubular plate. The defect was filled with a 40.0-mm PPF/TCP scaffold and collagen sponge overlaid as described above with (ORIF40 BMP; $n = 4$) or without (ORIF40 Cont; $n = 4$) 1.5 mg of BMP-2 impregnated in the sponge. The wounds were closed with Vicryl suture. The pigs were allowed free cage activity and ad lib access to food and water.

Radiographic Healing

We used the modified Radiographic Union Score for Tibia Fractures (mRUST) to quantify healing.[27] The mRUST assigns integer scores reflecting bone healing to four distinct cortices as follows: 1, no healing; 2, callus present but no cortical bridging; 3, bridging callus with fracture line remaining visible; and 4, bridging callus with no fracture line visible. The mRUST scores are determined on the anteroposterior (medial and lateral cortices) and lateral (anterior and posterior cortices) X-rays. Three orthopedic traumatologists graded the X-rays in a randomized blinded fashion on two separate occasions. The two observations from each surgeon were averaged, and mean mRUST scores were determined by averaging the three individual surgeon scores at each time point.

CT-based Healing

After euthanasia, tibias were dissected and internal fixation was removed for CT evaluation using a high-resolution CT scanner (XtremeCT II; Scanco Medical, Bruttisellen, Switzerland). The scanner produced a stack of 816 tomographic slices with a voxel size of 50 μm centered at the middle of the defect. The reconstructed tomographic images were imported into OsiriX MD 11.0.3 (Pixmeo SARL, Geneva, Switzerland) to create sagittal and coronal images spanning the defect site. Two observers reviewed sagittal and coronal plane reconstructions to determine the presence or absence of bone bridging involving the medial, lateral, anterior, and posterior cortices.

Torsion Testing

At the time of harvest, all soft tissues were removed. In IMN25 specimens, the proximal and distal crosslock screws were removed. In ORIF specimens, both plates and screws were removed. Specimens were stored at −20°C until testing.

Samples were thawed at room temperature for 24 hours before testing. The proximal end of the tibia was connected to a torque sensor (STS Torque Sensor, Largo, FL) and force gauge (Chantillon DFS Series Digital Force Gauge, Largo, FL) through a hex head screw inserted between the medial and lateral facets. Samples were then connected to a motorized torsional stand (Mark 10 TSTM-DC, Copiague, NY) connected to the digital controller (Mark 10 DC 4040, Copiague, NY). The samples were loaded at a torsional rate 0.05° per second to a maximum of 5° displacement. Torque-angle plots were recorded. We performed identical tests on the contralateral tibia for intact stiffness information. Maximum torque at failure or at 5°, whichever came first, divided by the maximum torque of the intact tibia at 5° was recorded.

Statistical Methods

We compared mRUST at monthly intervals between treatment groups. Mixed linear models were used to determine if there was a significant difference in ratings between the treatment groups, while also modeling the repeated measures structure and accounting for the within-rater covariance structure. Sensitivity analyses were performed using time as a covariate, rather than a random effect, to determine if this would attenuate the findings in the primary model that only included treatment. All analytic assumptions were verified, with fit statistics being used to determine that linear models were acceptable. All analyses were performed using SAS v9.4, SAS Institute, Cary, NC.

CT scanning was used to confirm cortical bridging and definitive healing. We compared the number of bridged cortices between groups. Torsion data were normalized to the intact contralateral tibia. Healed cortices by CT scanning and torsional data were compared between groups with standard t-tests.

RESULTS

Surgical Results

All IMN25 YMPs tolerated the surgery without complications. There were no early implant failures. One IMN25 Cont specimen was lame with gross implant failure at 3 months and was sacrificed. The other seven IMN25 Cont animals and all IMN25 BMP pigs made it to the 6-month euthanasia time point. Seven of eight of the IMN25 Cont pigs developed delayed wound breakdown and infection from 28 to 173 days after surgery. All were controlled with local debridement and oral antibiotics. One of the IMN BMP pigs developed an infection that was controlled with local debridement and oral antibiotics. Formal gait analysis was not performed, but by observation, none of the IMN25 Cont specimens resumed a normal gait pattern in contrast to IMN25 BMP specimens that were all walking without a limp by 2 months after surgery.

All four ORIF40 Cont pigs became lame in the 3rd postoperative month with obvious nonunions and were euthanized at 3 months. One of the ORIF40 BMP pigs became acutely lame 1 week after surgery with an obvious limb deformity and broken internal fixation and was euthanized early. The other three ORIF40 BMP pigs resumed normal gait patterns within 2 months of surgery, healed uneventfully, and were euthanized at 3 months postsurgery.

Radiographic Healing IMN YMPs

Healing trajectories in IMN25 Cont and IMN25 BMP pigs demonstrate early divergence in healing rates within the first

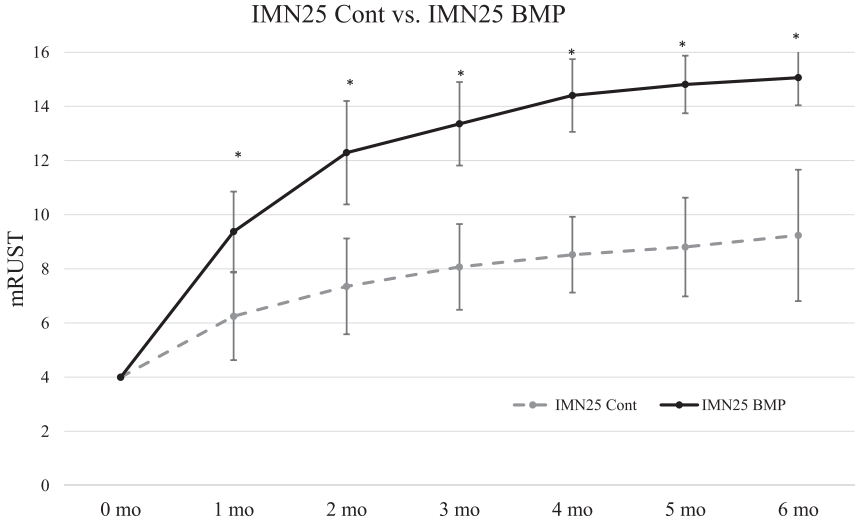

FIGURE 2. Modified Radiographic Union Score for Tibia fractures (mRUST) scoring of Yucatan minipigs treated with intramedullary nailing (IMN). Bone Morphogenetic Protein-2 (BMP-2) resulted in rapid radiographic healing in the 25.0-mm segmental bone defect model treated with an IMN as depicted by monthly mRUST scores (* denotes improved healing in IMN25 BMP with $P < .05$ compared to IMN25 Cont at that time point). All IMN25 BMP specimens were clinically and radiographically healed by 2-3 months. In contrast, the IMN25 Cont specimens had failed healing trajectories by 4 months, which did not improve.

month of injury (Fig. 2). X-rays of IMN25 Cont specimens at 2 and 6 months are shown in Supplementary Fig. S1, and corresponding CT cross-sections are shown in Supplementary Figure S2. Likewise, X-rays at 2 and 6 months in IMN25 BMP specimens are shown in Supplementary Figure S3, and CT cross-sections are shown in Supplementary Figure S4. By 2 months, all BMP specimens were radiographically healed (Supplementary Figs. S3 and S4). At 6 months, mRUST scores increased from 9.2 (±2.4) in IMN25 Cont to 15.1 (±1.0) in IMN25 BMP specimens ($P < .0001$). CT scanning demonstrated bridging callus on 30 of 32 possible cortices in BMP-2 specimens (Supplementary Fig. S4). Control specimens had no bridging callus in all 28 possible cortices (Supplementary Fig. S2).

Radiographic Healing ORIF40 YMPs

Healing trajectories in ORIF40 Cont and ORIF40 BMP pigs demonstrate similar early divergence in healing rates

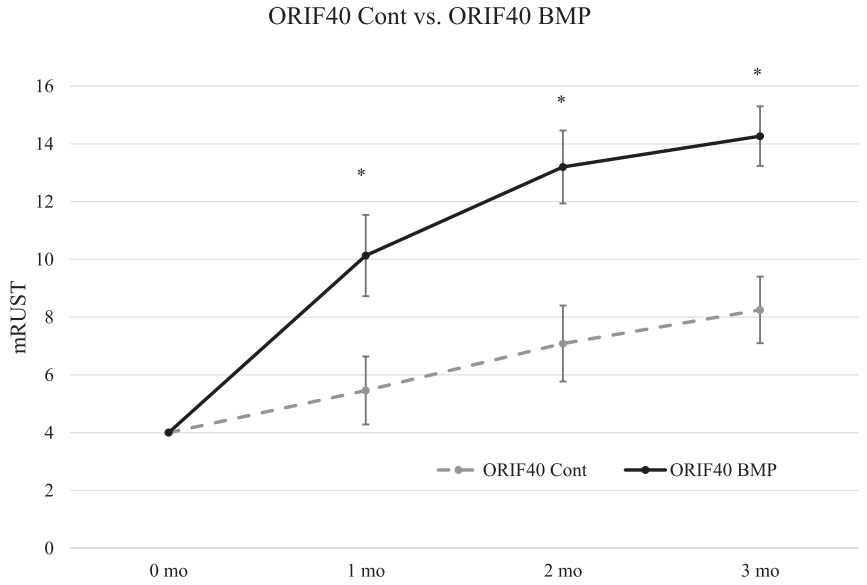

FIGURE 3. Modified Radiographic Union Score for Tibia fractures (mRUST) scoring of Yucatan minipigs treated with dual plating. Bone Morphogenetic Protein-2 (BMP-2) augmented radiographic healing in the 40.0-mm segmental bone defect model treated with an ORIF as depicted by monthly mRUST scores (* denotes improved healing in IMN25 BMP with $P < .05$ compared to IMN25 Cont at that time point). Three of four BMP specimens were clinically and radiographically healed by 2 months. The fourth specimen in the ORIF40 Cont group failed early and is not included in this analysis. None of the ORIF40 BMP specimens healed.

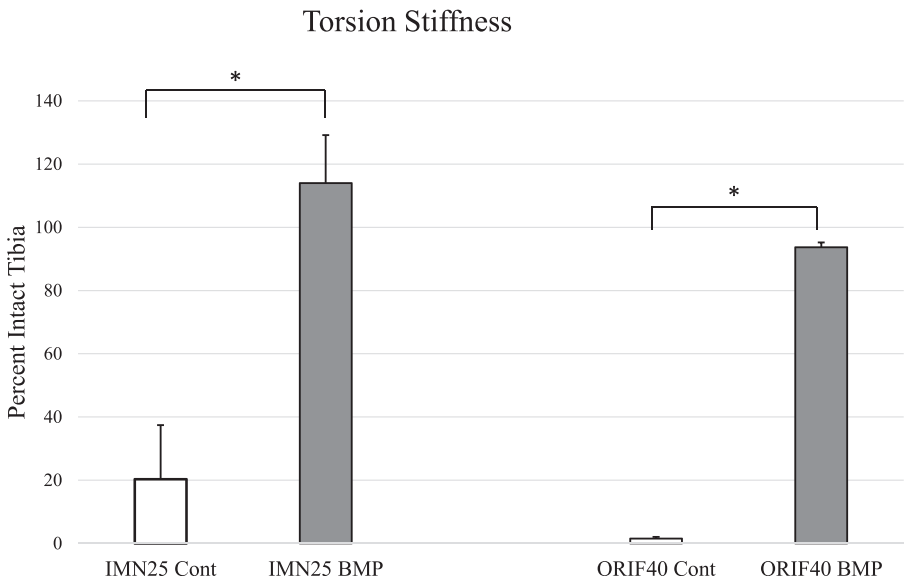

FIGURE 4. Torsional stiffness testing. Bone Morphogenetic Protein-2 (BMP-2)-treated animals had significantly increased torsional stiffness compared to untreated controls at the terminal time point in both IMN25 and ORIF40 groups (* denotes $P < 0.0001$ by standard t-test).

within the first month after injury (Fig. 3). X-rays of control and BMP-2 specimens at 3 months in the ORIF40 model are shown in Supplementary Figure S5. At 3 months after injury, mRUST scores increased from 8.2 (±1.2) in ORIF40 Cont specimens to 14.3 (±1.0) in ORIF40 BMP specimens ($P < .01$). CT scanning (Supplementary Fig. S6) confirmed bridging callus seen on 11 of 12 possible cortices in ORIF40 BMP specimens.

Torsion Testing

Torsion testing confirmed radiographic findings with the restoration of intact stiffness in the IMN25 BMP and ORIF40 BMP groups (Fig. 4). In contrast, controls regained very little torsional stiffness in either model.

DISCUSSION

In our original model development, we investigated 25-mm defects stabilized with IMN, which led to a CSD but with concomitant delayed wound breakdown.[19] We changed to dual plating to augment torsional stability (ORIF25 Cont conditions), and these animals healed without wound complications. Accordingly, we increased the defect to 40 mm in dual-plated specimens (ORIF40 Cont conditions), which clearly led to early fixation failure and a CSD. In the current experiment, BMP-2 rescued bone healing in both CSD models. BMP-2 has been shown to facilitate bone healing in multiple small animal,[25–27] translational,[8,13] and clinical[28–30] bone healing models. In the IMN25 YMPs, untreated SBDs did not heal and there was consistent delayed wound breakdown. We hypothesize that wound breakdown resulted from nonunion instead of causing nonunion. Addition of BMP-2 into the SBD clearly accelerated bone healing and prevented wound breakdown in IMN25 YMPs. The 40.0-mm defect was a severe insult as evidenced by gross failure in all ORIF40 Cont animals by 3 months even with dual plating. Again, BMP-2 was effective to heal these large defects. The effects of BMP-2 on bone healing were rapid in both CSD models, with clear divergence in healing trajectories in the first month after injury (Figs. 2 and 3). In early clinical work, BMP-2 reduced the number of secondary operations and reduced infections in patients sustaining open tibial fractures.[31] In subsequent studies, it has continued to show efficacy in achieving bony union in several clinical models.[28–30] Our studies appear to be consistent with both the reduced infection rate and the ability of BMP-2 treatment to result in a bony union.

Porcine models offer several advantages compared to other translational SBD models. Porcine models share notable immunologic[15–17,20,21] and metabolic fidelity[32] with humans when sustaining extremity trauma and hemorrhagic shock. This is likely important as a significant number of mangled limbs occur in multiply injured patients. In addition, the majority of polytrauma models investigating systemic metabolic and immunologic responses have been done in porcine models.[20,21] Accordingly, the immunologic response likely affects bone and soft tissue healing and should be accounted for in translational injury models. While there are numerous porcine polytrauma models, there is a lack of corresponding extremity injury investigations in porcine models. A functioning porcine extremity injury model is particularly adaptable to investigate extremity war injuries as concomitant injuries that include damage to overlying muscle and skin, additional visceral injuries, traumatic brain injuries, and hemorrhagic shock are all common in warfighters who sustain severe limb injuries.[33,34] However, it needs to be recognized that surgical resection of a SBD in this model does not reproduce extremity war injury conditions that would include damage to the adjacent soft tissue and typically a concussive wave from a blast mechanism that significantly expands the zone of injury.

There are several existing porcine weight-bearing diaphyseal SBD models. Our model development indicates a threshold for a CSD lies between 25.0 and 40.0 mm in dual-plated specimens. Runyan and colleagues demonstrated that a 30-mm SBD treated with dual plating healed by 16 weeks in juvenile breeder pigs consistent with our model.[19,35] However, they used skeletally immature pigs. Lin and colleagues created 30.0-mm femur SBDs in Taiwan Lee-Sung minipigs and treated them with a locking plate.[36] Defects treated with adipose stem cells carrying a genetically engineered vector were rescued and were on a healing trajectory. Untreated defects did not heal and were filled with fibrous tissue. Our models compare favorably to the work of Runyan and Lin. The dual-plated specimens in Runyan's model[35] healed at a similar rate to our specimens in model development.[19] In contrast, single-plated preparations described by Lin[36] would have significantly less torsional resistance, and the authors report no bone healing in untreated defects.

There are several limitations with our study. Seven of eight of the IMN25 Cont animals had wound breakdown that possibly resulted from chronic limb instability from a nonunion. It is also distinctly possible that the nonunions in this group resulted from infection. However, seven of eight IMN25 BMP specimens, subjected to an identical defect and fixation methods, had no wound complications and rapid bone healing. Taken together, it is more plausible that wound breakdown was secondary to residual limb instability, but this is not known. Specimen numbers in the ORIF40 groups are small and will need more experimentation to support our preliminary findings. However, all control animals had gross failure. In contrast, three of four of the BMP-2 animals healed robustly, and the fourth animal failed within a week, which was not related to nonunion. In studies quantifying plain radiographic bone healing, mRUST scores have become the gold standard, but they have moderate inter- and intra-rater reproducibility.[27,37–39] Three trained observers made two independent blinded readings of the X-rays in this study. Our interclass coefficients for inter and intra-rater reliability were approximately 0.8, demonstrating the utility of this index. In addition, mRUST scores corresponded well with torsion testing and were validated by CT-based findings.

Finally, although BMP-2 has been shown to be an effective osteoinductive bone healing intervention in multiple studies, the goal of this study was to further validate both of our porcine CSD models using a known bone healing intervention as a "positive" control.

CONCLUSIONS

In summary, BMP-2 reliably healed two different CSD in the tibia of YMPs. The onset of action of BMP is rapid and begins during the first month of healing. The porcine model is a novel option for bone defect research and offers a translational model with excellent fidelity to human injury response.

ACKNOWLEDGMENTS

We thank James Slaven for statistical support for the project. We also acknowledge support from the National Institutes of Health (NIH/NIAMS P30 AR072581; Principal Investigator Sharon Moe MD) and the Indiana Clinical Translational Science Award/Institute (NCATS UL1TR002529-01).

SUPPLEMENTARY MATERIAL

Supplementary material is available at *Military Medicine* online.

FUNDING

Research reported in this publication was primarily supported by the The Department of Defense USAMRMC W81XWH-13-1-0407, W81XWH-13-1-0500, W81XWH-13-1-0501;. National Institutes of Health (NIH/NIAMS P30 AR072581) and the Indiana Clinical Translational Science Award/Institute (NCATS UL1TR002529-01).

CONFLICT OF INTEREST STATEMENT

None of the authors have any conflicts of interest pertaining to the content of this manuscript.

REFERENCES

1. Konda SR, Gage M, Fisher N, Egol KA: Segmental bone defect treated with the induced membrane technique. J Orthop Trauma 2017; 31(Suppl 3): S21–2.
2. McClure PK, Alrabai HM, Conway JD: Preoperative evaluation and optimization for reconstruction of segmental bone defects of the tibia. J Orthop Trauma 2017; 31(Suppl 5): S16–9.
3. Betz OB, Betz VM, Nazarian A, et al: Direct percutaneous gene delivery to enhance healing of segmental bone defects. J Bone Joint Surg Am 2006; 88(2): 355–65.
4. Piacentini F, Ceglia MJ, Bettini L, Bianco S, Buzzi R, Campanacci DA: Induced membrane technique using enriched bone grafts for treatment of posttraumatic segmental long bone defects. J Orthop Traumatol 2019; 20(1): 13.
5. McKinley TO, D'Alleyrand JC, Valerio I, Schoebel S, Tetsworth K, Elster EA: Management of mangled extremities and orthopaedic war injuries. J Orthop Trauma 2018; 32(Suppl 1): S37–42.
6. Pearce AI, Richards RG, Milz S, Schneider E, Pearce SG: Animal models for implant biomaterial research in bone: a review. Eur Cell Mater 2007; 13: 1–10.
7. Cong Z, Jianxin W, Huaizhi F, Bing L, Xingdong Z: Repairing segmental bone defects with living porous ceramic cylinders: an experimental study in dog femora. J Biomed Mater Res 2001; 55(1): 28–32.
8. Decambron A, Fournet A, Bensidhoum M, et al: Low-dose BMP-2 and MSC dual delivery onto coral scaffold for critical-size bone defect regeneration in sheep. J Orthop Res 2017; 35(12): 2637–45.
9. Kruyt MC, Dhert WJ, Yuan H, et al: Bone tissue engineering in a critical size defect compared to ectopic implantations in the goat. J Orthop Res 2004; 22(3): 544–51.
10. Pobloth AM, Checa S, Razi H, et al: Mechanobiologically optimized 3D titanium-mesh scaffolds enhance bone regeneration in critical segmental defects in sheep. Sci Transl Med 2018; 10(423): 127–30.
11. Rozen N, Bick T, Bajayo A, et al: Transplanted blood-derived endothelial progenitor cells (EPC) enhance bridging of sheep tibia critical size defects. Bone 2009; 45(5): 918–24.
12. Segal U, Shani J: Surgical management of large segmental femoral and radial bone defects in a dog: through use of a cylindrical titanium mesh cage and a cancellous bone graft. Vet Comp Orthop Traumatol 2010; 23(1): 66–70.
13. Zhu L, Chuanchang D, Wei L, Yilin C, Jiasheng D: Enhanced healing of goat femur-defect using BMP7 gene-modified BMSCs and load-bearing tissue-engineered bone. J Orthop Res 2010; 28(3): 412–8.
14. Thorwarth M, Schultze-Mosgau S, Kessler P, Wiltfang J, Schlegel KA: Bone regeneration in osseous defects using a resorbable nanoparticular hydroxyapatite. J Oral Maxillofac Surg 2005; 63(11): 1626–33.
15. Horst K, Eschbach D, Pfeifer R, et al: Local inflammation in fracture hematoma: results from a combined trauma model in pigs. Mediators Inflamm 2015; 2015: 126060.
16. Horst K, Hildebrand F, Pfeifer R, et al: Impact of haemorrhagic shock intensity on the dynamic of alarmins release in porcine poly-trauma animal model. Eur J Trauma Emerg Surg 2016; 42(1): 67–75.
17. Serve R, Sturm R, Schimunek L, et al: Comparative analysis of the regulatory T cells dynamics in peripheral blood in human and porcine polytrauma. Front Immunol 2018; 9: 435.
18. McKinley TO, Lisboa FA, Horan AD, Gaski GE, Mehta S: Precision medicine applications to manage multiply injured patients with orthopaedic trauma. J Orthop Trauma 2019; 33(Suppl 6): S25–9.
19. McKinley TO, Natoli RM, Fischer JP, et al: Internal fixation construct and defect size affect healing of a translational porcine diaphyseal tibial segmental bone defect. Mil Med 2020.
20. Hildebrand F, Andruszkow H, Huber-Lang M, Pape HC, von Griensven M: Combined hemorrhage/trauma models in pigs-current state and future perspectives. Shock 2013; 40(4): 247–73.
21. Hildebrand F, Weuster M, Mommsen P, et al: A combined trauma model of chest and abdominal trauma with hemorrhagic shock—description of a new porcine model. Shock 2012; 38(6): 664–70.
22. Valparaiso AP, Vicente DA, Bograd BA, Elster EA, Davis TA: Modeling acute traumatic injury. J Surg Res 2015; 194(1): 220–32.
23. Kadhim M, Holmes L Jr., Gesheff MG, Conway JD: Treatment options for nonunion with segmental bone defects: systematic review and quantitative evidence synthesis. J Orthop Trauma 2017; 31(2): 111–9.
24. Chu TM, Warden SJ, Turner CH, Stewart RL: Segmental bone regeneration using a load-bearing biodegradable carrier of Bone Morphogenetic Protein-2. Biomaterials 2007; 28(3): 459–67.
25. Einhorn TA, Majeska RJ, Mohaideen A, et al: A single percutaneous injection of recombinant human Bone Morphogenetic Protein-2 accelerates fracture repair. J Bone Joint Surg Am 2003; 85(8): 1425–35.
26. Pearson HB, Mason DE, Kegelman CD, et al: Effects of Bone Morphogenetic Protein-2 on neovascularization during large bone defect regeneration. Tissue Eng Part A 2019; 25(23-24): 1623–34.
27. Litrenta J, Tornetta P 3rd, Mehta S, et al: Determination of radiographic healing: an assessment of consistency using RUST and modified RUST in metadiaphyseal fractures. J Orthop Trauma 2015; 29(11): 516–20.
28. Dai J, Li L, Jiang C, Wang C, Chen H, Chai Y: Bone Morphogenetic Protein for the healing of tibial fracture: a meta-analysis of randomized controlled trials. PLoS One 2015; 10(10): e0141670.
29. Lyon T, Scheele W, Bhandari M, et al: Efficacy and safety of recombinant human Bone Morphogenetic Protein-2/calcium phosphate matrix for closed tibial diaphyseal fracture: a double-blind, randomized,

controlled phase-II/III trial. J Bone Joint Surg Am 2013; 95(23): 2088–96.
30. Rearick T, Charlton TP, Thordarson D: Effectiveness and complications associated with recombinant human Bone Morphogenetic Protein-2 augmentation of foot and ankle fusions and fracture nonunions. Foot Ankle Int 2014; 35(8): 783–8.
31. Govender S, Csimma C, Genant HK, et al: Recombinant human Bone Morphogenetic Protein-2 for treatment of open tibial fractures: a prospective, controlled, randomized study of four hundred and fifty patients. J Bone Joint Surg Am 2002; 84(12): 2123–34.
32. Clendenen N, Nunns GR, Moore EE, et al: Hemorrhagic shock and tissue injury drive distinct plasma metabolome derangements in swine. J Trauma Acute Care Surg 2017; 83(4): 635–42.
33. Howard JT, Kotwal RS, Stern CA, et al: Use of combat casualty care data to assess the US military trauma system during the Afghanistan and Iraq conflicts, 2001-2017. JAMA Surg 2019; 154(7): 600–8.
34. Vasquez KB, Brozoski FT, Logsdon KP, Chancey VC: Retrospective analysis of injuries in underbody blast events: 2007-2010. Mil Med 2018; 183(supplemental 1): 347–52.
35. Runyan CM, Vu AT, Rumburg A, et al: Repair of a critical porcine tibial defect by means of allograft revitalization. Plast Reconstr Surg 2015; 136(4): 461e–73e.
36. Lin CY, Wang YH, Li KC, et al: Healing of massive segmental femoral bone defects in minipigs by allogenic ASCs engineered with FLPo/Frt-based baculovirus vectors. Biomaterials 2015; 50: 98–106.
37. Cekic E, Alici E, Yesil M: Reliability of the radiographic union score for tibial fractures. Acta Orthop Traumatol Turc 2014; 48(1): 533–40.
38. Fiset S, Godbout C, Crookshank MC, Zdero R, Nauth A, Schemitch E: Experimental validation of the Radiographic Union Score for Tibial Fractures (RUST) using micro-computed tomography scanning and biomechanical testing in an in-vivo rat model. J Bone Joint Surg Am 2018; 100(25): 1871–8.
39. Litrenta J, Tornetta P 3rd, Ricci W, et al: In vivo correlation of radiographic scoring (radiographic union scale for tibia fractures) and biomechanical data in a sheep osteotomy model: can we define union radiographically? J Orthop Trauma 2017; 31(3): 127–30.